



# Simulating Nonequilibrium Transport Processes of Ammonium Through Unsaturated Sandy Soil

Chaoshuo Hou · Wei Xiu · Mengmeng He

Received: 21 March 2021 / Accepted: 21 October 2021 / Published online: 8 November 2021  
© The Author(s), under exclusive licence to Springer Nature Switzerland AG 2021

**Abstract** Transport of nitrogen compounds to groundwater, especially from agricultural fertilization, is a main problem in aquifer contamination. Ammonium ( $\text{NH}_4^+\text{-N}$ ) is one of the most common nitrogen fertilizer forms. In order to evaluate the risk of agricultural fertilizer pollution to aquifers caused by infiltration, a soil column experiment and breakthrough modeling simulation were employed to study  $\text{NH}_4^+\text{-N}$  retention by a sandy soil profile (10–60 cm depth). The soil used was collected from an irrigated semi-arid cropland in Bulanghe Town, Yuyang District, Yulin City, Shaanxi Province of China, and recombined in a laboratory soil column. Column experiments were accomplished using aqueous solutions containing various concentrations of  $\text{NH}_4^+\text{-N}$  and the breakthrough curves were determined. The linear soil-water partition coefficients ( $K_d$ ) were

determined from batch equilibrium experiments, and the retardation factor ( $R_d$ ) for the saturated sandy soil was computed. The lowest  $\text{NH}_4^+\text{-N}$  concentrations at the depth range of 10–20 cm suggested the strongest  $\text{NH}_4^+\text{-N}$  sorption. The chemical nonequilibrium model in Hydrus-1D can better simulate the breakthrough of  $\text{NH}_4^+\text{-N}$  through the soil column. The soil sorption capacity decreases as the irrigation flow rate increases. The results provide a scientific basis for optimization of fertilizer application in agricultural management under irrigation in desert oasis, and those semi-arid areas with similar soil texture and vadose zones of small thickness.

**Keywords** Ammonia fertilization · Groundwater contamination · Sorption · Sandy soil · Flow rate · Hydrus-1D

C. Hou · M. He  
School of Water Resources and Environment, China University of Geosciences (Beijing), Beijing 100083, People's Republic of China

W. Xiu  
State Key Laboratory of Biogeology and Environmental Geology, China University of Geosciences (Beijing), Beijing 100083, People's Republic of China

W. Xiu (✉)  
Institute of Earth Sciences, China University of Geosciences (Beijing), Beijing 100083, People's Republic of China  
e-mail: xwsuron@cugb.edu.cn

## 1 Introduction

Ammonium ( $\text{NH}_4^+\text{-N}$ ) has become a common contaminant in groundwater (Liang et al., 2020; Perović et al., 2020). The  $\text{NH}_4^+\text{-N}$  contamination in aquifers under farmland is mainly the result of applying manure or of N-bearing fertilizer components, but it is also caused by percolation of pretreated wastewater which is used for aquifer recharge (Li et al., 2020; Liang et al., 2020; Perović et al., 2020). Ammonium is generally regarded as a key parameter for the

evaluation of groundwater contamination risk (Yang et al., 2017).

The nitrogen level is a significant indicator of soil fertility. In some intensive crop production areas in China, excessive N fertilization has caused serious environmental problems, which are related to the enrichment of water and soil, and atmospheric enrichment with active forms of  $N_2O$  (Yan et al., 2014; Zhou et al., 2018). Therefore, in experiments to quantify  $NH_4^+$ -N pollution which reaches groundwater from farmland and determine the efficiency of different porous media that reduces the contaminant through absorption, it is proved that clay particles in soils are a major stock of  $NH_4^+$  (Jellali et al., 2010). Thus, conducting a study on the  $NH_4^+$ -N sequestration in sandy soils containing low amount of clay minerals is essential, considering that there are only a limited number of such studies so far published.

Process-based or deterministic models are used to explore the transport processes or spatial distribution of solute in groundwater assessment on a regional or local scale (Kuntz & Grathwohl, 2009). For simulation of such processes, analytical solution of the convection-dispersion equation model (CDEM) can adequately describe the movement of solute at least in laboratory columns filled with macroscopically homogeneous soil. However, for heterogeneous soils, the traditional transport model simulation will deviate significantly from experimental results (Gaber et al., 1995). The measured breakthrough curve (BTC) usually features early arrival and obvious long tailing due to the varying scales of the intrinsic heterogeneity of soils. The development of chemical nonequilibrium models (CNEMs) proved to better simulate solute migration in heterogeneous soils. It is presumed that adsorption occurs not only instantaneously at easily accessible adsorption sites, but also with slow kinetics at less accessible ion exchange sites (Henrichs et al., 2009; Jellali et al., 2010; Wang et al., 2013; Ngo et al., 2014).

Ammonium transport processes in sandy soils in the columns can be better captured by a one-site CNEM according to a comparative study of the performance of the CDEM and CNEM carried out by Jellali et al. (2010). Ramos et al. (2011) studied  $NH_4^+$ -N migration in soils irrigated with salt water, finding that Hydrus-1D is a useful software for analyzing solute migration of nitrogen species. The discrepancy of  $NH_4^+$ -N concentrations between

simulation and measurement is due to the equilibrium model rather than the nonequilibrium model used in the simulation (Ramos et al., 2011). However, there are few comparative studies conducted to reveal the differences of these two models (CDEM, one-site CNEM) for simulation of  $NH_4^+$ -N transport in semi-arid soil. Thus, a controlled experiment is necessary to compare the performance of these two models.

According to Ishikawa et al. (2003),  $NH_4^+$ -N concentrations in water percolating paddy fields will decrease as the percolation rates decrease, which means that a lower percolation rate might increase the contact time and as a result enhance the soil's ability to absorb  $NH_4^+$ -N. Jellali et al. (2010) reported similar findings when they studied ammonium adsorption by sandy soil in fixed bed columns. To our knowledge, there is no such a research about ammonia adsorption effects of irrigation flow rates on sandy soil using these models.

The purposes of this study were to (i) study the adsorption and migration of  $NH_4^+$ -N in the sandy soil of semi-arid Yuyang District, Shaanxi Province of China, through batch and column experiments, (ii) draw a comparison between the performances of the CDEM and one-site CNEM for expressing  $NH_4^+$ -N solute migration process via a soil column, and (iii) analyze effect of flow rate on the  $NH_4^+$ -N transport. Taking into account the fertilizer scheme performed in Bulanghe Town of Yuyang District, laboratory column experiments using sandy soils collected in the field were conducted to analyze the migration process of  $NH_4^+$ -N. The experimental results were analyzed with Hydrus-1D to study the effect of flow rate and fit the breakthrough curves (BTCs).

## 2 Materials and Methods

### 2.1 Experimental Materials

In the "Mu Us Sandy Land" oases, tens of hectares of sandy soil (based on the USDA textural soil classification system) are utilized for irrigated cropping fed from groundwater to support the population in Uxin Qi, Inner Mongolia, and Yuyang district, Shaanxi Province of China. The total irrigation in the studied area is as high as 300-570 mm year<sup>-1</sup>, primarily as the form of the flood irrigation method. Typical nitrogen fertilizer application rates are about 350 kgN

ha<sup>-1</sup> in this region, exceeding nitrogen fertilizer need of 200 kgN ha<sup>-1</sup> (Li et al., 2016) in this China's district. As the local soil texture is lighter, excess irrigation and fertilizer applications result in extensive water loss and nitrogen leakage through drainage. Based on investigation conducted by Li et al. (2014), the standard rate excess of ammonium, nitrate, and nitrite nitrogen in groundwater is high in the Mu Us Sandy Land area. Moreover, the Hailiutu River catchment has a classic monsoonal climate with exceeding 74% of annual rainfall concentrated in summer (Hou et al., 2018). The traditional practice of local farmers is to spread N fertilizer on the surface of soil before the flood irrigation or heavy rainfall events resulting in water and fertilizer flow rate increasing and most N leaching in summer in this region, and this can add the risk of groundwater nitrate pollution. Physical properties of the soil at the experimental site are given in Table 1. The average porosity was estimated at  $0.353 \pm 0.014$ , and the pH was  $8.20 \pm 0.65$ . The cation exchange capacity was  $4.89 \pm 0.63$  cmol kg<sup>-1</sup> and the mean soil organic matter content was  $3.73 \pm 2.99$  g kg<sup>-1</sup>. The contents of ammonia and total nitrate in the soil at the time of sampling were  $6.81 \pm 2.73$  and  $22.57 \pm 17.22$  mg kg<sup>-1</sup>, respectively.

## 2.2 Batch Equilibrium Experiment

A batch equilibrium experiment was used to establish the ammonia absorption coefficients of various layers of soils. The initial concentrations of ammonium used in the batch sorption study were 10, 50, 100, 150, 200, and 250 mg L<sup>-1</sup>, respectively. The method considering impact of solute concentration under higher rainfall intensity on the solute transport was similar to those studies of Pot et al. (2005) and Mastrocicco

et al. (2019). An aliquot of 5 g of soil layer material was put into a 50-mL test tube with ammonium chloride mixtures containing different experimental conditions for NH<sub>4</sub><sup>+</sup>-N concentrations. In the following steps, those samples were shaken using a temperature-controlled oscillator at 175 rpm and  $20 \pm 1$  °C. After 48 h of equilibration, the tubes were centrifuged and supernatants were collected. The concentration of NH<sub>4</sub><sup>+</sup>-N in the supernatant solutions was analyzed using a Bioblock Scientific distiller via nitrogen distillation analysis method. On the basis of batch adsorption study results, the adsorption isotherms of NH<sub>4</sub><sup>+</sup>-N on the sand soil texture were analyzed regressively by using three types of adsorption models, i.e., Freundlich model, Langmuir model, and linear model (data not shown). The sorption behavior could be represented by the following linear distribution model formula:

$$C_s = C_w K_d \quad (1)$$

where  $C_s$  (mg kg<sup>-1</sup>) and  $C_w$  (mg L<sup>-1</sup>) represent the concentration of sorbate on sorbent and the equilibrium solution NH<sub>4</sub><sup>+</sup>-N concentration, respectively;  $K_d$  (L kg<sup>-1</sup>) denotes the soil-water distribution coefficient. The linear distribution model fitted well to the results of batch adsorption experiment, with  $r^2$  in the range of 0.98–0.99.

## 2.3 Soil Column Test

### 2.3.1 Experiment Apparatus

The test device (Fig. 1) for the ammonium migration experiment includes a cylindrical plexiglass column (70 cm high and 12 cm inner diameter), filled with

**Table 1** Soil physical properties

| Soil layer depth range (cm) | Bulk density ( $\rho$ ) (g cm <sup>-3</sup> ) | Particle size distribution |                       |                         | USDA soil texture | Soil moisture at saturation ( $\theta_{sat}$ , cm <sup>3</sup> cm <sup>-3</sup> ) | Organic matter (%) | CEC (cmol kg <sup>-1</sup> ) |
|-----------------------------|---|----------------------------|-----------------------|-------------------------|-------------------|---|--------------------|------------------------------|
|                             |   | Clay (%) 10nm-2 $\mu$ m    | Silt (%) 2-50 $\mu$ m | Sand (%) 50 $\mu$ m-2mm |                   |   |                    |                              |
| 0–10                        | 1.39  | 0.28                       | 12.32                 | 87.41                   | Sand              | 0.369   | 6.97               | 4.95                         |
| 10–20                       | 1.41  | 0.4                        | 13.01                 | 86.59                   | Sand              | 0.355   | 7.83               | 4.72                         |
| 20–30                       | 1.57  | 0.73                       | 17.27                 | 82.00                   | Sand              | 0.363   | 3.67               | 5.75                         |
| 30–40                       | 1.56  | 0.22                       | 10.67                 | 89.11                   | Sand              | 0.360   | 1.39               | 5.19                         |
| 40–50                       | 1.58  | 0.12                       | 8.49                  | 91.39                   | Sand              | 0.335   | 1.19               | 4.87                         |
| 50–60                       | 1.60  | 0.08                       | 5.47                  | 94.45                   | Sand              | 0.337   | 1.36               | 3.83                         |

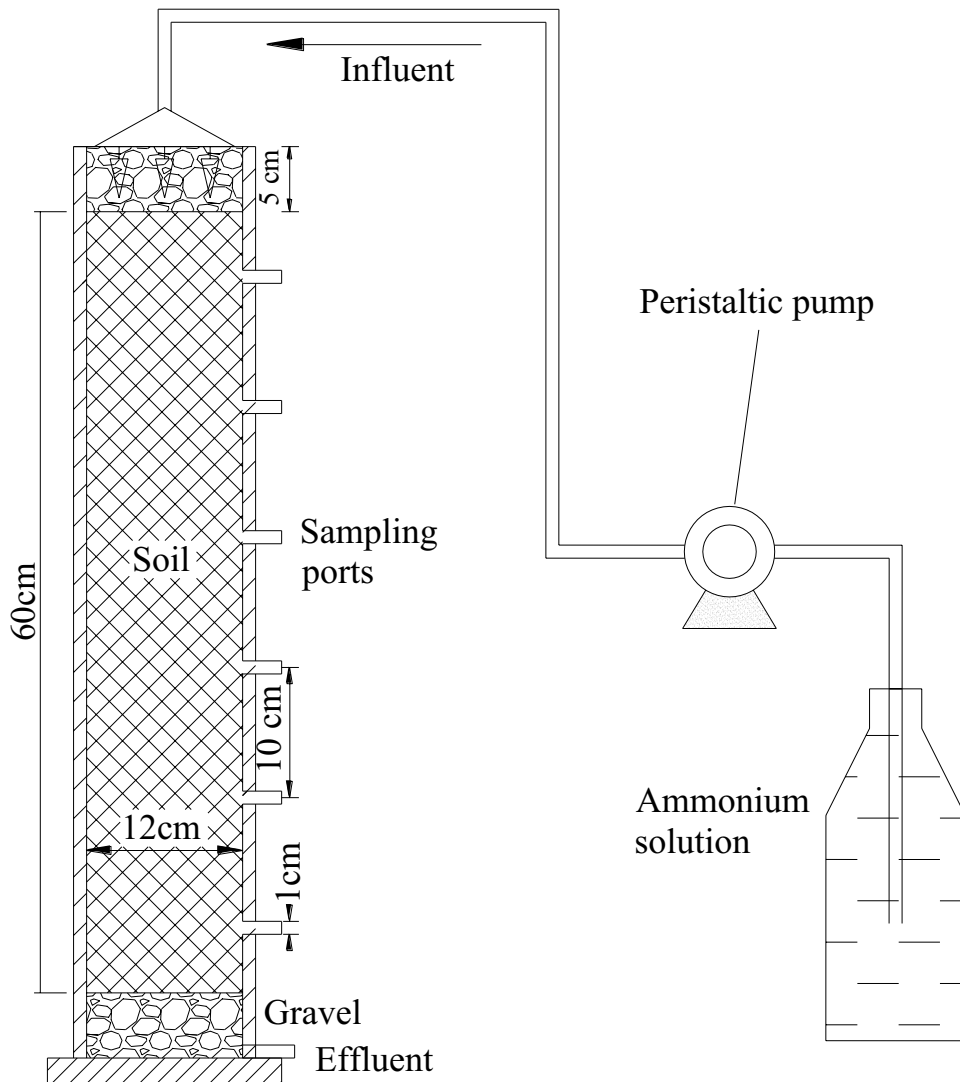


**Fig. 1** Experimental device for ammonium transport research

6 layers of soil gathered from the Bulanghe Town and compressed homogeneously individually based on the actual bulk density of each original soil layer (Table 1). The thickness of each layer is about 10 cm. Gravel layers of 5-cm thickness were utilized at the top and bottom boundaries of the column to insure appropriate water drainage. The soil column was first rinsed with deionized water until no ammonia concentrations were detected as impurities. The inflow solution was then applied via a sprinkler continuously on the top of the column with a flow rate adjusted to  $2.5 \text{ mL min}^{-1}$  by means of a peristaltic pump (Baoding Longer Precision Pump Co., China). The pH was

kept at 8.2 and the temperature was maintained at  $20 \pm 0.2 \text{ }^\circ\text{C}$  during the experiments.

The column flow of  $2.5 \text{ mL min}^{-1}$  was determined based on the amount of fertilizer rate and irrigation depth used by local farmers and precipitation intensity in this area (i.e.,  $0.22 \text{ mm min}^{-1}$ ). The diameter of the soil column is 12 cm. The flow rates ( $\text{mL min}^{-1}$ ) were computed according to the irrigation rate or precipitation intensity ( $\text{mm min}^{-1}$ ) and the cross-sectional area of soil column. The flow rates fixed for the experimental and subsequent modeling study are shown in Table 2. Teflon-coated Rhizon soil moisture samplers at various depths from the column soil

**Table 2** The flow rates for the experimental and modeling study

|   | Irrigation rate or precipitation intensity |                          | Rate of flow (mL min <sup>-1</sup> ) |
|---|--|--------------------------|--------------------------------------|
|   | (mm min <sup>-1</sup> )                    | (mm hour <sup>-1</sup> ) |                                      |
| 1 | 0.13                                       | 7.96                     | 1.50                                 |
| 2 | 0.22                                       | 13.20                    | 2.50                                 |
| 3 | 0.44                                       | 26.53                    | 5.00                                 |
| 4 | 0.88                                       | 53.05                    | 10.00                                |
| 5 | 1.32                                       | 79.58                    | 15.00                                |

surface (5, 15, 25, 35, 45, and 55 cm) were submerged to collect the soil water at the six side ports. Solution samples from side ports of the column were sampled to analyze depth-dependent solute concentrations.

### 2.3.2 Ammonium Migration Experiment

Equivalent ammonium application rate through nitrogen fertilization is about 350 kgN ha<sup>-1</sup> in the study region, which exceeds N fertilizer requirement of 200 kgN ha<sup>-1</sup> in its growing period (Li et al., 2016). In this column research, we chose 100 kgN ha<sup>-1</sup> fertilizer each time, assuming water input (precipitation + irrigation) during growing season was about 5 mm each time. Therefore, the equivalent dissolved NH<sub>4</sub><sup>+</sup> application on the column soil surface was chosen at NH<sub>4</sub><sup>+</sup>-N concentration of 150 mg L<sup>-1</sup>. Accordingly, an inflow ammonium with NH<sub>4</sub><sup>+</sup>-N concentration of 50 mg L<sup>-1</sup> was applied for model calibration, and with NH<sub>4</sub><sup>+</sup>-N concentration of 150 mg L<sup>-1</sup> for model validation and for study of flow rate effect. The stock solutions were prepared by dissolving ammonium sulfate ((NH<sub>4</sub>)<sub>2</sub>SO<sub>4</sub>) in 1.0 L of distilled water. Throughout the experiment, the flow rate was kept at 2.5 mL min<sup>-1</sup>, which corresponded to a column flow velocity of 0.22 mm min<sup>-1</sup>.

Although the nitrate and nitrite concentrations of samples from column ports were measured, these concentrations were still lower than their observation limits (0.08 mg N L<sup>-1</sup> and 0.003 mg N L<sup>-1</sup>, respectively), which indicated nitrification rates can be negligible during the experiment. In this study, only the sorption of ammonia nitrogen by the soil was considered, while nitrification was neglected considering it has little impact at this relatively short contact time. Moreover, no experiment replication was done

owing to the large size of the column but with six side observation holes. This was consistent with other studies using experimental setups with similar sizes (Jellali et al., 2010).

## 2.4 Model Description

### 2.4.1 Equilibrium Transport Model

According to Section 2.2, it is assumed that there is a linear relation between the solid and solute phase concentrations. The equilibrium CDE model is the most common and basic mathematical model to describe solute transport and retention under steady-state flow conditions as follows (Pot et al., 2005; Zhou et al., 2019; Guelfo et al., 2020; Li et al., 2021):

$$\theta R \frac{\partial c}{\partial t} = \theta D \frac{\partial^2 c}{\partial Z^2} - q \frac{\partial c}{\partial z} - \mu_w \theta c \quad (2)$$

where  $t$  (min) and  $z$  (cm) represent the time and the space coordinates, respectively;  $\theta$  is the water content (cm<sup>3</sup> cm<sup>-3</sup>);  $q$  is the Darcian water flux (cm min<sup>-1</sup>);  $D$  denotes the dispersion coefficient (cm<sup>2</sup> min<sup>-1</sup>);  $\mu_w$  represents first-order degradation constant (min<sup>-1</sup>), which is not considered in the present study;  $R$  denotes the retardation factor:

$$R = 1 + \frac{\rho K_d}{\theta} \quad (3)$$

where  $\rho$  denotes the bulk density (g cm<sup>-3</sup>).

The hydrodynamic dispersion coefficient  $D$  is as follows:

$$D = \frac{q}{\theta} \alpha_L \quad (4)$$

where  $\alpha_L$  denotes the longitudinal dispersivity (cm).

### 2.4.2 Nonequilibrium Transport Model

It takes time for the sorbate to reach a concentration equilibrium in the sorption process, so the CNEM is used on the basis of a kinetic sorption process. This nonequilibrium transport-controlled state usually occurs when the interaction between the sorbent and the solute is slower than the residence time of the solute in the transport process. The sorption sites on the surface of soil particles are divided into instantaneous equilibrium sites (adsorption type I, commonly

variable surface charge sites) and first-order kinetic sorption sites (type II, commonly fixed charge ion exchange sites) (van Genuchten & Wagenet, 1989; Henrichs et al., 2009; Jellali et al., 2010; Wang et al., 2013; Zhou et al., 2019).

The nonequilibrium sorption-desorption reaction has been considered by this two-site sorption model. It is assumed that there are two kinds of sorption sites (van Genuchten & Wagenet, 1989):

$$S_T = S_1 + S_2 \quad (5)$$

where  $S_T$  represents the total adsorption capacity (mg  $\text{mg}^{-3}$ ); sorption site  $S_1$  is supposed to be instantaneous, whereas  $S_2$  is considered to be a kinetically hindered ion exchange site. The first-order kinetic equation for the type-2 site without degradation is given as:

$$\frac{\partial S_2}{\partial t} = \mu [(1-f)K_d C - S_2] \quad (6)$$

where  $C$  denotes the solute concentration (mg  $\text{cm}^{-3}$ );  $f$  represents the ratio of the exchange site to the solute concentration in equilibrium (-), which is zero for the one-site CNEM;  $\mu$  denotes the first-order rate coefficient ( $\text{min}^{-1}$ ).

If a linear soil-water distribution coefficient was applied, the transport equation for the two-site sorption process is (Šimůnek & Van Genuchten, 2013; Zhou et al., 2019)

$$\frac{\partial(\theta C)}{\partial t} + \rho \frac{\partial S_1}{\partial t} + \rho \frac{\partial S_2}{\partial t} = \frac{\partial}{\partial z} \left( \theta D \frac{\partial C}{\partial z} \right) - \frac{\partial(qC)}{\partial z} \quad (7)$$

$$S_1 = fK_d C \quad (8)$$

The Hydrus-1D code (Šimůnek et al., 2013; Wang et al., 2015) was selected to solve the transport equations (Eqs. (2), (6), (7), and (8)) for the  $\text{NH}_4^+$ -N transport process in this experiment.

### 2.4.3 Boundary Conditions

The model flow domain reached down to 60 cm below the column surface, discretized into 60 slices with a constant size of 1 cm.

The upper and the lower boundary were defined as atmospheric boundary and free drainage conditions for water flow, respectively.

The  $\text{NH}_4^+$ -N migration in the soil column was simulated under unsaturated flow conditions as considered by the water content ( $\theta$ ), which is the fraction of the total soil filled with liquid water and must be less than the total porosity  $n$ . The water content is very important in vadose zone hydrology, where the hydraulic conductivity is a strongly nonlinear function of water content, but complicates the solution of the unsaturated groundwater flow equation.

The ammonium inflow rate was calculated according to the water flow rate and liquid concentration at the upper boundary of the column. The lower initial boundary condition was set to zero concentration. It was thus supposed that the soil and water in the column did not contain  $\text{NH}_4^+$  ions initially.

### 2.4.4 Model Input Parameters

The pore connectivity was supposed to be 0.5, while the saturated soil-water content ( $\theta_s = n$ ) was measured for the same soil, so as to decrease the number of soil hydraulic parameters in the model calibration. The residual water content ( $\theta_r$ ), saturated hydraulic conductivity ( $K_{\text{sat}}$ ), and other model parameters ( $\alpha$ ,  $n$ ) were acquired by the Rosetta method using bulk density and soil textural distribution as inputs (Table 3).

The initial longitudinal dispersivity ( $a_L$ ) was set at 0.5 cm as default in the HYDRUS code. The initial  $K_d$  values were used on the basis of the linear isotherms obtained from batch equilibrium experiments (see Sections 2.2 and 3.1). The CDEM with parameter optimization module in Hydrus-1D was used to determine the values of  $a_L$  and  $K_d$  using column side port  $\text{NH}_4^+$ -N concentration data with an inflow  $\text{NH}_4^+$ -N concentration of 50  $\text{mg}^{-1}$  L, similar to the approach used by Hu et al. (2008) and Wang et al. (2014). By this, the  $a_L$

**Table 3** Hydraulic parameters of six soil layers of the test column in the Hydrus-1D model

| Soil depths (m) | $\theta_r$ ( $\text{m}^3 \text{m}^{-3}$ ) | $\alpha$ ( $\text{m}^{-1}$ ) | $n$   | $k_{\text{sat}}$ (cm $\text{min}^{-1}$ ) | $l$ |
|-----------------|---|------------------------------|-------|--|-----|
| 0–10            | 0.041                                     | 0.044                        | 2.301 | 0.270                                    | 0.5 |
| 10–20           | 0.044                                     | 0.040                        | 2.705 | 0.372                                    | 0.5 |
| 20–30           | 0.048                                     | 0.035                        | 3.531 | 0.477                                    | 0.5 |
| 30–40           | 0.049                                     | 0.034                        | 3.699 | 0.550                                    | 0.5 |
| 40–50           | 0.048                                     | 0.034                        | 3.687 | 0.530                                    | 0.5 |
| 50–60           | 0.049                                     | 0.033                        | 3.866 | 0.599                                    | 0.5 |



value for the NH<sub>4</sub><sup>+</sup>-N transport simulation at different concentrations and flow rates was obtained.

### 2.4.5 Optimization Algorithm

In soil science and hydrology, parameter optimization on the basis of the Levenberg-Marquardt algorithm has been widely applied (e.g., Pot et al., 2005; Ngo et al., 2014). After selecting the initial parameter choice, the Levenberg-Marquardt nonlinear minimization was used for parameter optimization on the basis of the minimization of the target function  $\varphi$  (Ngo et al., 2014):

$$\varphi(b) = \sum_{i=1}^{\beta} \sigma_i [O_i(t_i) - S_i(t_i, b)]^2 \tag{9}$$

where  $i$  and  $\beta$  are the ordinal number of time steps and the total number of observations, respectively;  $O_i(t_i)$  and  $S_i(t_i, b)$  are observations at time  $t_i$  and the corresponding simulated space-time values, respectively;  $\sigma_i$  denotes a weighting factor set to unity in this study.

### 2.5 Model Performance Criteria

The experimental datasets were employed to calibrate and validate the model similar as reported by Hao et al. (2014) and Wang et al. (2014, 2015). The NH<sub>4</sub><sup>+</sup>-N concentrations measured in various soil layers were applied to calibrate solute transport parameters.

In order to validate the model results, the following three criteria were applied to quantify the deviation of the modeling results from the observed concentrations:

$$r = \frac{\sum_{i=1}^N (C_{ie} - \bar{C}_{ie})(C_{io} - \bar{C}_{io})}{\sqrt{\sum_{i=1}^N (C_{ie} - \bar{C}_{ie})^2 \sum_{i=1}^N (C_{io} - \bar{C}_{io})^2}} \tag{10}$$

$$RMSE = \sqrt{\frac{1}{N} \sum_{i=1}^N (C_{io} - C_{ie})^2} \tag{11}$$

$$RE = \left| \frac{\sum_{i=1}^N C_{ie}}{\sum_{i=1}^N C_{io}} - 1 \right| \tag{12}$$

where  $C_{io}$  and  $C_{ie}$  represent the  $i$ th observed NH<sub>4</sub><sup>+</sup>-N concentration and the  $i$ th model-guessed NH<sub>4</sub><sup>+</sup>-N concentration;  $\bar{C}_{io}$  and  $\bar{C}_{ie}$  are the mean value of  $C_{io}$

and the average value of  $C_{ie}$ ;  $N$  denotes the number of observations at a specific observation site;  $r$  denotes correlation coefficient; RMSE denotes root mean squared error; and RE is the relative error.

### 2.6 Effect of Flow Rate

Furthermore, the calibrated and validated model parameters were used to evaluate the effect of the irrigation flow rate on ammonium sorption by the sandy soil, based on the fixed inlet NH<sub>4</sub><sup>+</sup>-N concentration of 150 mg L<sup>-1</sup>. Five independent simulation models were adopted to evaluate the influence of the bed contact time on its adsorption ability. The flow rates were fixed to 1.5, 2.5, 5, 10, and 15 mL min<sup>-1</sup> (Table 2). The contact times between dissolved NH<sub>4</sub><sup>+</sup>-N and the soil matrix were 6334, 3764, 1840, 885, and 569 min, and Darcy’s velocities were 0.013, 0.022, 0.044, 0.088, and 0.132 cm min<sup>-1</sup>, respectively.

## 3 Results and Discussions

### 3.1 Adsorption Isotherms

The adsorption isotherms are depicted in Fig. 2, and the adsorption behavior can in fact be represented by formula (1). The linear model fitted well with  $r^2$  of between 0.98 and 0.99 ( $C_S = 1.707C_e$ ,  $r^2 = 0.984$ ;  $C_S = 6.361C_e$ ,  $r^2 = 0.980$ ;  $C_S = 2.029C_e$ ,  $r^2 = 0.982$ ;  $C_S = 1.985C_e$ ,  $r^2 = 0.979$ ;  $C_S = 1.976C_e$ ,  $r^2 = 0.991$ ;  $C_S = 4.687C_e$ ,  $r^2 = 0.984$ , at the sand soil depth ranges of 0-10, 10-20, 20-30, 30-40, 40-50, and 50-60 cm, respectively). It was found that the linear model is the most appropriate for fitting the experimental data, so it could well describe the adsorption process of NH<sub>4</sub><sup>+</sup>-N for the Bulanghe soil. The distribution coefficients of 1.71, 6.36, 2.03, 1.98, 1.98, and 4.69 L kg<sup>-1</sup> were attained at the soil depth ranges of 0-10, 10-20, 20-30, 30-40, 40-50, and 50-60 cm, respectively, in these batch adsorption experiments.

During model alignment, these distribution coefficients were employed as the initial estimates, and were calibrated according to the experimental concentrations of NH<sub>4</sub><sup>+</sup>-N transport in the column.

An average  $K_d$  value of 3.13 L kg<sup>-1</sup> was computed using Eq. 1 (Fig. 2). These comparatively small  $K_d$  values obtained from the batch equilibrium test are

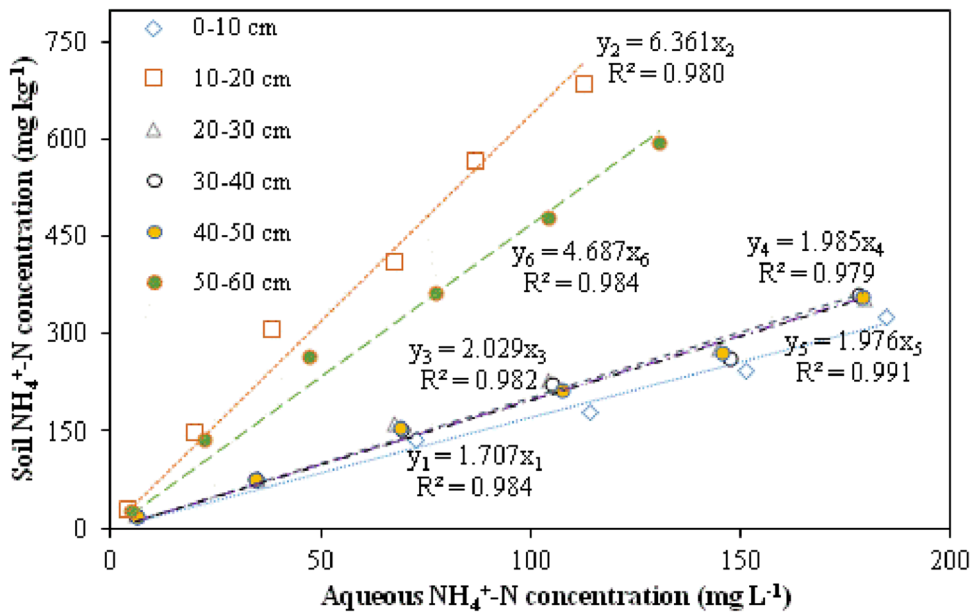


**Fig. 2** Ammonium sorption isotherms for sandy soil fitted with linear  $K_d$  model

consistent with the sandy soil of low sorption capacity used in the test, which contains low level of organic matter and clay content (Table 1) mainly responsible for  $\text{NH}_4^+\text{-N}$  adsorption. Retardation factor in a saturated soil ( $R_d$ ), taken as an equilibrium retardation factor, was computed by formula  $R_d = 1 + \frac{\rho K_d}{p}$ , where  $p$  denotes the porosity. Retardation factors of 7.44, 26.26, 9.79, 9.59, 10.34, and 23.30 were thus determined for the soil depth ranges of 0-10, 10-20, 20-30, 30-40, 40-50, and 50-60 cm, respectively. The maximum value of retardation factor appears in the soil at the medium depth of 10-20 cm, which shows that this layer has the strongest sorption capacity for  $\text{NH}_4^+\text{-N}$ . Ishikawa et al. (2003) reported similar finding about  $\text{NH}_4^+\text{-N}$  adsorption relating to constant area with the soil particles, when they studied the adsorption on  $\text{NH}_4^+\text{-N}$  in paddy soil percolation water.

### 3.2 Breakthrough Curves

At the outset of the column experiment, the  $\text{NH}_4^+\text{-N}$  sorption rate was comparatively high, but after reaching the sorption-desorption equilibrium, the sorption rate went down to almost zero (Fig. 3). This phenomenon is related to the decrease in the utilization of the

sorption sites and the change of the solute concentration gradient.

### 3.3 Model Calibration and Validation for Simulation of $\text{NH}_4^+\text{-N}$ Migration

The experiment results at 10, 20, 30, 40, 50, and 60 cm soil depths with inlet  $\text{NH}_4^+\text{-N}$  concentration of  $50 \text{ mg L}^{-1}$  were used for model calibration. The solute transport parameters ( $a_L$ ,  $K_d$ ,  $\mu$ ) were calibrated as shown in Table 4. Compared with the CDEM, the one-site CNEM gives slightly optimal predicting results, as illustrated by the bigger  $r$  and smaller RMSE values of the one-site CNEM than those of the CDEM in simulating the  $\text{NH}_4^+\text{-N}$  transport via the soil column (Table 5).

Parameters obtained from the experiment with the optimization algorithm were applied to verify the model for the alternative experimental data (Wang et al., 2015). To that end, when the model was calibrated by matching the column water and  $\text{NH}_4^+\text{-N}$  transport data with an inlet  $\text{NH}_4^+\text{-N}$  concentration of  $50 \text{ mg L}^{-1}$  (Table 5), it is necessary to use the column experiment BTC with the inlet  $\text{NH}_4^+\text{-N}$  concentration of  $150 \text{ mg L}^{-1}$  to further verify the model. In the following steps, the calibrated



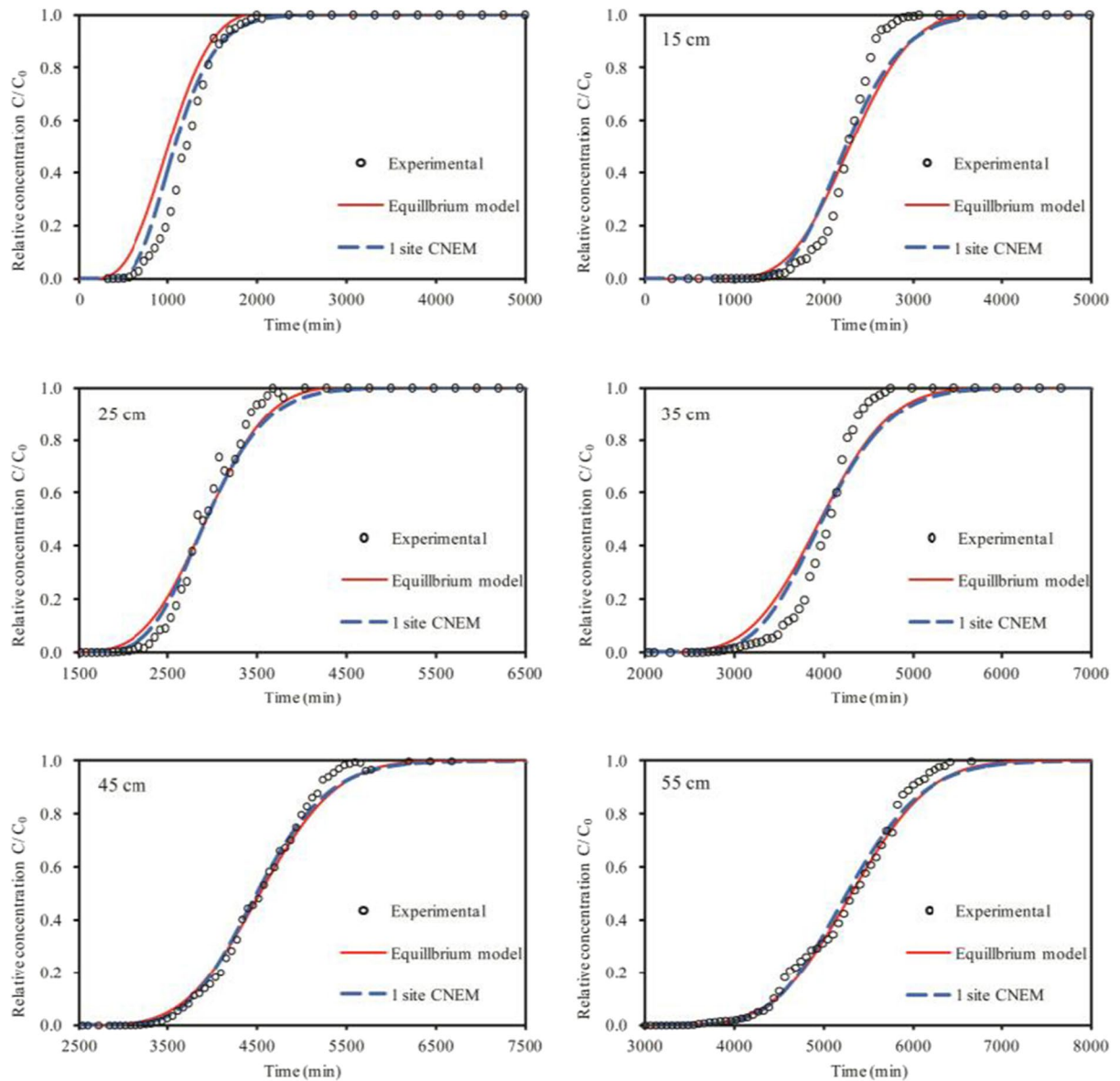


**Fig. 3** Observed and fitted BTCs at various soil column depths of the ammonium migration experiment at a flow rate of  $2.5 \text{ mL min}^{-1}$  with inlet  $\text{NH}_4^+\text{-N}$  concentration of  $150 \text{ mg L}^{-1}$

models, CDEM and one-site CNEM, were used to simulate the BTCs of experiments with inlet  $\text{NH}_4^+\text{-N}$  concentration of  $150 \text{ mg L}^{-1}$ . Results demonstrated that  $r$ , RMSE, and RE indices in the verification simulation were quite near (and in some cases better) to alignment values (Table 6). Therefore, the calibrated model was validated.

### 3.4 Comparison of Fitting Results by the Two Models

The experimental  $C/C_0$  with inlet  $\text{NH}_4^+\text{-N}$  concentration of  $150 \text{ mg L}^{-1}$ , with values guessed by the CDEM (Eq. 2) and CNEM (Eqs. 6, 7, and 8), are shown in Fig. 4 (a and b). All BTCs evaluated by the CDEM showed to be earlier than the experimental

**Table 4** Solute transport parameter ( $K_d$ ) of the CDEM, along with  $K_d$  and  $\mu$  values for the one-site CNEM ( $e$ , estimated parameters)

| Soil depth range (cm) | Parameter estimates |                               |             |                               |                            |
|-----------------------|---------------------|-------------------------------|-------------|-------------------------------|----------------------------|
|                       | CDEM                |                               | 1-site CNEM |                               |                            |
|                       | $a_L^e$ (cm)        | $K_d^e$ (L kg <sup>-1</sup> ) | $a_L^e$     | $K_d^e$ (L kg <sup>-1</sup> ) | $M^e$ (min <sup>-1</sup> ) |
| 0–10                  | 0.258               | 3.049                         | 0.258       | 3.055                         | 0.180                      |
| 10–20                 | 0.411               | 0.537                         | 0.411       | 0.884                         | 0.202                      |
| 20–30                 | 0.140               | 1.150                         | 0.140       | 1.080                         | 0.099                      |
| 30–40                 | 0.638               | 1.394                         | 0.638       | 1.367                         | 0.078                      |
| 40–50                 | 0.204               | 0.065                         | 0.204       | 0.157                         | 0.284                      |
| 50–60                 | 0.157               | 1.967                         | 0.157       | 1.711                         | 0.045                      |

**Table 5** Values of  $r$ , RMSE, and RE as indicators of simulation accuracy for the CDEM and one-site CNEM (calibration approach)

| Depth in soil (m) | Simulation model |       |        |             |       |        |
|-------------------|------------------|-------|--------|-------------|-------|--------|
|                   | CDEM             |       |        | 1-site CNEM |       |        |
|                   | $r$              | RMSE  | RE     | $r$         | RMSE  | RE     |
| 0.05              | 0.994            | 0.042 | 0.008  | 0.989       | 0.055 | 0.015  |
| 0.15              | 0.993            | 0.043 | -0.014 | 0.979       | 0.098 | -0.069 |
| 0.25              | 0.989            | 0.075 | 0.050  | 0.992       | 0.065 | -0.044 |
| 0.35              | 0.773            | 0.250 | -0.196 | 0.968       | 0.133 | -0.153 |
| 0.45              | 0.988            | 0.065 | 0.123  | 0.997       | 0.040 | -0.047 |
| 0.55              | 0.996            | 0.043 | -0.070 | 0.990       | 0.112 | -0.260 |
| mean              | 0.956            | 0.086 | -0.017 | 0.986       | 0.084 | -0.093 |
| Min <sup>a</sup>  | 0.773            | 0.042 | -0.196 | 0.968       | 0.040 | -0.260 |
| Max <sup>b</sup>  | 0.996            | 0.250 | 0.123  | 0.997       | 0.133 | 0.015  |
| Std <sup>c</sup>  | 0.089            | 0.081 | 0.109  | 0.011       | 0.036 | 0.098  |

<sup>a</sup>Represents the minimum value

<sup>b</sup>Represents the maximum value

<sup>c</sup>Represents the standard deviation

**Table 6** Values of  $r$ , RMSE, and RE for simulated results of NH<sub>4</sub><sup>+</sup>-N concentration (verification approach)

| Depth in soil (m) | Simulation model |       |        |             |       |        |
|-------------------|------------------|-------|--------|-------------|-------|--------|
|                   | CDEM             |       |        | 1-site CNEM |       |        |
|                   | $r$              | RMSE  | RE     | $r$         | RMSE  | RE     |
| 0.05              | 0.994            | 0.050 | 0.022  | 0.994       | 0.042 | 0.012  |
| 0.15              | 0.987            | 0.065 | -0.024 | 0.991       | 0.055 | -0.010 |
| 0.25              | 0.993            | 0.044 | -0.021 | 0.995       | 0.036 | -0.015 |
| 0.35              | 0.987            | 0.064 | -0.011 | 0.988       | 0.062 | -0.010 |
| 0.45              | 0.997            | 0.036 | -0.051 | 0.999       | 0.022 | -0.016 |
| 0.55              | 0.998            | 0.034 | -0.082 | 0.996       | 0.027 | -0.027 |
| mean              | 0.992            | 0.049 | -0.028 | 0.994       | 0.041 | -0.011 |
| Min <sup>a</sup>  | 0.987            | 0.034 | -0.082 | 0.988       | 0.022 | -0.027 |
| Max <sup>b</sup>  | 0.998            | 0.065 | 0.022  | 0.999       | 0.062 | 0.012  |
| Std <sup>c</sup>  | 0.005            | 0.013 | 0.036  | 0.004       | 0.016 | 0.013  |

<sup>a</sup>Represents the minimum value

<sup>b</sup>Represents the maximum value

<sup>c</sup>Represents the standard deviation

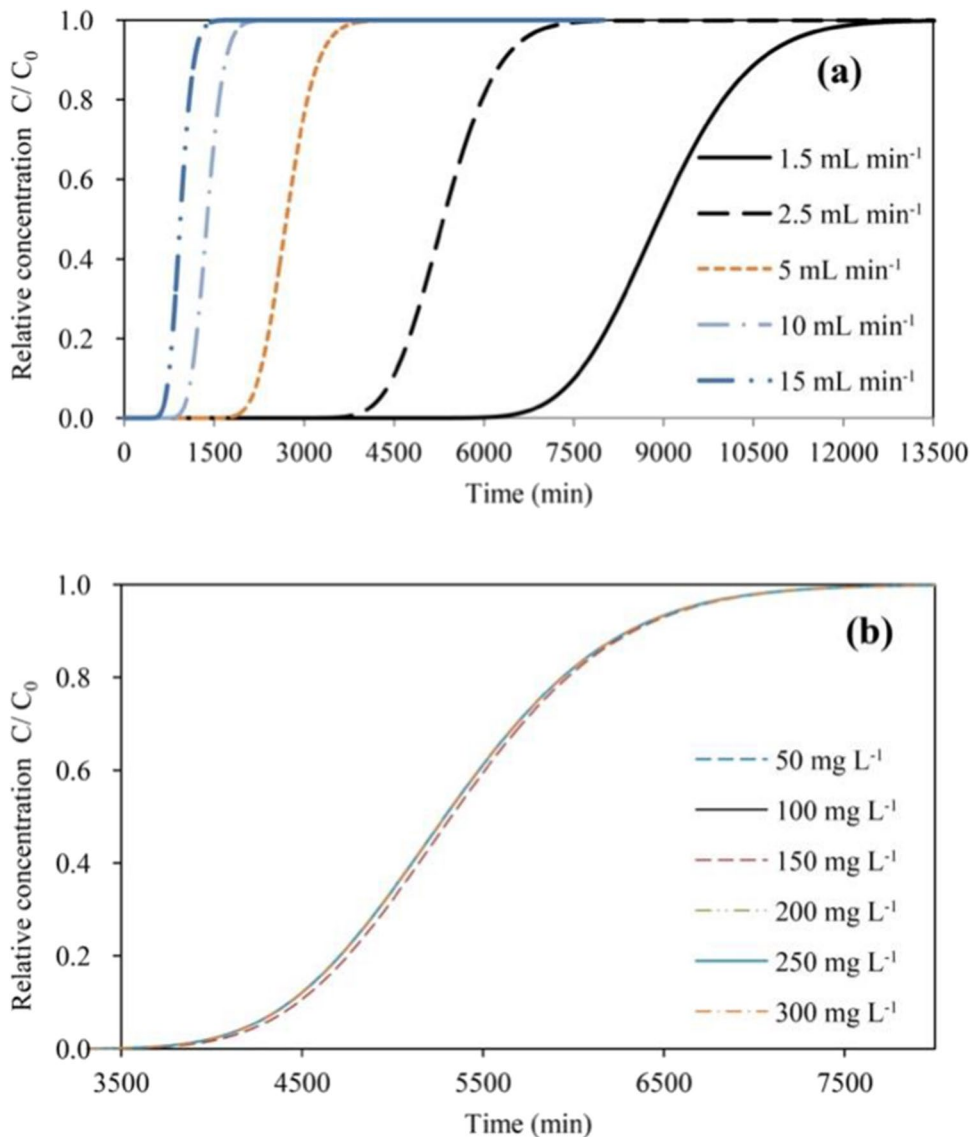


**Fig. 4** Fitted breakthrough curves (one-site CNEM) of ammonium for various irrigation flow rates ( $C_0, \text{NH}_4^+\text{-N} = 150 \text{ mg L}^{-1}$ ) (a), and various concentration of ammonium (flow rate  $2.5 \text{ mL min}^{-1}$ ) (b)

column transport data at their initial stages. Therefore, the CDEM cannot well simulate the sorption process of  $\text{NH}_4^+\text{-N}$ , indicating that the migration of  $\text{NH}_4^+\text{-N}$  in the model is faster than that in the column experiments. Compared with the migration velocity of  $\text{NH}_4^+\text{-N}$  solute, the CDEM cannot adequately simulate the slowness of  $\text{NH}_4^+\text{-N}$  sorption reaction, which is similar to the study of Ramos et al. (2011). This slow adsorption rate might be caused by the

diffusion process of colloidal clay particles during the formation of aggregate.

The BTCs simulated by the one-site CNEM ( $f = 0$ ) are pretty reasonable with the  $\text{NH}_4^+\text{-N}$  adsorption experimental values (Fig. 3), demonstrating that the one-site CNEM simulates the experimental results quite well. In comparison with the CDEM, the CNEM demands an extra parameter,  $\mu$ , which features the sorption kinetics (Tables 5 and 6). High  $\mu$  values indicate faster equilibria of  $\text{NH}_4^+$  between the liquid and

solid phases, while lower  $\mu$  values show slower equilibration (Šimůnek & Van Genuchten, 2008). At the depth ranges of 0–10, 10–20, 20–30, 30–40, 40–50, and 50–60 cm, the  $\mu$  values of the one-site CNEM were 0.180, 0.202, 0.099, 0.078, 0.284, and 0.045  $\text{min}^{-1}$ , respectively. These values were similar to (or slightly lower than) the values of Jellali et al. (2010), where  $\mu$  values range from 0.0596 to 0.1110  $\text{min}^{-1}$ . A lower  $\mu$  means less adsorption of ammonium caused by the slowed down equilibration of the solute between the liquid and solid phases, and resulted in earlier solute arrivals (Simunek & Van Genuchten, 2008). Therefore, the ammonium migration from aqueous solution to soil matrix is also limited in this study.

### 3.5 Impact of Irrigation Flow Rate

The flow condition at the top boundary in the model was changed to simulate ammonium sorption under different irrigation flow conditions. The validated parameters as mentioned above were used. The BTCs of  $\text{NH}_4^+\text{-N}$  acquired for the five irrigation flow rates (1.5, 2.5, 5, 10, and 15  $\text{mL min}^{-1}$ ) are shown in Fig. 4a demonstrating a decrease of  $\text{NH}_4^+\text{-N}$  adsorption onto the soil matrix with an increase in irrigation flow rate and, consequently, a decrease in the bed contact time. As a matter of fact, the adsorption decreased from 138, 137, 134, to 129, and finally to 124  $\text{mg kg}^{-1}$  for an irrigation flow rate increase from 1.5, 2.5, 5, to 10, and finally to 15  $\text{mL min}^{-1}$ , and thus a bed contact time decrease from 6334, 3764, 1840, to 885, and finally to 569 min. Sprynskyy et al. (2005), Sarioglu (2005), Khorsha and Davis (2017), and Fronczyk and Markowska-Lech (2021) reported similar findings when they studied the sorption of ammonium by local Ukrainian, Turkish zeolites, aluminosilicate aggregates and low-cost mineral materials as zeolite, limestone sand, and halloysite. For instance, Sarioglu (2005) found a reduction in the sorption ability of approximately 40% when the flow rate increases from 0.5 to 4  $\text{mL min}^{-1}$ . Therefore, the sorption efficiency decreases when the flow rate increases related to fertilizer apply before flood irrigation or big rainfall. Fitted breakthrough curves (one-site CNEM) of various concentrations of ammonium are shown in Fig. 4b. A comparison of the results from Fig. 4a and Fig. 4b indicates that the influence of the various irrigation

flow rates on breakthrough curve was greater than that of the concentration of ammonium.

Booker et al. (1996) showed that reducing the velocity could enhance the performance of the column bed media up to a certain limit, and noted that  $\text{NH}_4^+\text{-N}$  removal by clinoptilolite is mostly due to ion exchange, and allowing longer contact times facilitated the cations to reach the interlayer exchange sites within the clinoptilolite structure, thereby enhancing ammonium removal. Khorsha and Davis (2017) also found that columns operating at higher velocities of 42  $\text{cm h}^{-1}$  had relatively low removal efficiency compared to those at 8.3  $\text{cm h}^{-1}$  due to facilitating sorption in their column.

## 4 Conclusions

Transport of ammonium ( $\text{NH}_4^+\text{-N}$ ), one of the most common nitrogen fertilizer forms, to groundwater from agricultural fertilization, is a main problem in aquifer contamination. In this study, the Hydrus-1D code was employed to simulate the  $\text{NH}_4^+\text{-N}$  transport and breakthrough curves in columns filled with sandy soil taken from a farmland site (Bulanghe Town) of a desert oasis.

- (1) According to the batch adsorption experimental data, the linear  $K_d$  relationship can well represent the  $\text{NH}_4^+\text{-N}$  sorption process by the sandy soil. For the  $\text{NH}_4^+\text{-N}$  column laboratory tests, the sigmoidal BTCs have certain asymmetry. The column test results show that nonequilibrium sorption occurring during the migration is responsible for this asymmetry.
- (2) In the column experiment, the one-site CNEM presented better simulation results than the CDEM for the  $\text{NH}_4^+\text{-N}$  breakthrough curves. The low first-order kinetic sorption rate resulted in the rapid  $\text{NH}_4^+\text{-N}$  leaching in the soil.
- (3) The adsorption capacity of  $\text{NH}_4^+\text{-N}$  on the sandy soil increases as the irrigation flow rate decreases.

The present experimental and simulation results help to optimize the fertilizer application in agricultural management under irrigation in desert oasis, and those semi-arid areas with similar soil texture and vadose zones of small thickness. However, given

the low possibility of natural ammonium attenuation in the studied sandy soil, further study combining the mathematical model with field experiment would be helpful to illuminate the impact of rainfall/irrigation intensity on the leaching of ammonium to groundwater and to determine the maximum fertilization rate so that the soil will retain ammonium under normal soil-water content.

**Acknowledgements** We thank Michael Kersten for his extensive comments on the first draft of this paper.

**Author Contribution** C.S. Hou, W. Xiu, and M.M. He have contributed to the text development and have given approval to the final version of the manuscript. W. Xiu led the work and C.S. Hou shaped an early version of the text.

**Funding** The study was financially supported by the National Natural Science Foundation of China (41702272, 41861144027).

**Data Availability** The datasets used and/or analyzed during the current study are available from the corresponding author on reasonable request.

#### Declarations

**Ethics Approval and Consent to Participate** Not applicable.

**Consent for Publication** Not applicable.

**Conflict of Interest** The authors declare no competing interests.

#### References

- Booker, N. A., Cooney, E. L., & Priestley, A. J. (1996). Ammonia removal from sewage using natural Australian zeolite. *Water Science and Technology*, 34(9), 17–24.
- Fronczyk, J., & Markowska-Lech, K. (2021). Treatment efficiency of synthetic urban runoff by low-cost mineral materials under various flow conditions and in the presence of salt: Possibilities and limitations. *Science of The Total Environment*. <https://doi.org/10.1016/j.scitotenv.145199>
- Gaber, H. M., Inskeep, W. P., Comfort, S. D., & Wraith, J. M. (1995). Nonequilibrium transport of atrazine through large intact soil cores. *Soil Science Society of America Journal*, 59(1), 60–67.
- Guelfo, J. L., Wunsch, A., McCray, J., Stults, J. F., & Higgins, C. P. (2020). Subsurface transport potential of perfluoroalkyl acids (PFAAs): Column experiments and modeling. *Journal of Contaminant Hydrology*, 233, 103661.
- Hao, Y. Y., Xu, X., Huang, Q. Z., & Huang, G. H. (2014). Modeling soil water-salt dynamics and maize yield responses to groundwater depths and irrigations. *Transactions of the Chinese Society of Agricultural Engineering*, 30(20), 128–136 (in Chinese with English abstract).
- Henrichs, M., Welker, A., & Uhl, M. (2009). Modelling of bio-filters for ammonium reduction in combined sewer overflow. *Water Science and Technology*, 60(3), 825–831.
- Hou, L. Z., Hu, B. X., Li, H., & Wan, L. (2018). Potential impacts of climate variation on potato field evapotranspiration: Field experiment and numerical simulation of potato water use in an arid site. *Journal of Geophysical Research – Atmospheres*, 123, 10202–10214.
- Hu, K. L., Li, B. G., Chen, D. L., Zhang, Y. P., & Edis, R. (2008). Simulation of nitrate leaching under irrigated maize on sandy soil in desert oasis in Inner Mongolia, China. *Agriculture Water Management*, 95, 1180–1188.
- Ishikawa, M., Tabuchi, T., & Yamaji, E. (2003). Clarification of adsorption and movement by predicting ammonia nitrogen concentrations in paddy percolation water. *Paddy and Water Environment*, 1, 27–33.
- Jellali, S., Diamantopoulos, E., Kallali, H., Bennaceur, S., Anane, M., & Jedidi, N. (2010). Dynamic sorption of ammonium by sandy soil in fixed bed columns: Evaluation of equilibrium and non-equilibrium transport processes. *Journal of Environmental Management*, 91(4), 897–905.
- Khorsha, G., & Davis, A. P. (2017). Ammonium removal from synthetic stormwater using clinoptilolite and hydroaluminosilicate columns. *Water Environment Research*, 564–575.
- Kuntz, D., & Grathwohl, P. (2009). Comparison of steady-state and transient flow conditions on reactive transport of contaminants in the vadose soil zone. *Journal of Hydrology*, 369(3–4), 225–233.
- Liang, Y., Ma, R., Wang, Y. X., Wang, S., Qu, L., Wei, W. H., & Gan, Y. Q. (2020). Hydrogeological controls on ammonium enrichment in shallow groundwater in the central Yangtze River Basin. *Science of The Total Environment*, 741, 140350.
- Li, J., Guo, K., Cao, Y. S., Wang, S. S., Song, Y., & Zhang, H. B. (2021). Enhance in mobility of oxytetracycline in a sandy loamy soil caused by the presence of microplastics. *Environmental Pollution*, 269, 116151.
- Li, Q., Wang, W. K., & Fu, G. J. (2014). The situation and trends analysis of shallow groundwater quality in the blown - sand region of the northern Shaanxi province. *Journal of Arid Land Resources and Environment*, 28(12), 94–98 (in Chinese with English abstract).
- Li, S., Yang, M., Wang, H., & Zhao, Y. (2020). Dynamic characteristics of immobilized microorganisms for remediation of nitrogen-contaminated groundwater and high-throughput sequencing analysis of the microbial community. *Environmental Pollution*, 267, 114875.
- Li, Y., Liu, H. J., & Huang, G. H. (2016). The effect of nitrogen rates on yields and nitrogen use efficiencies during four years of wheat–maize rotation cropping seasons. *Agronomy Journal*, 108(5), 2076–2088.
- Mastrociccio, M., Colombani, N., Soana, E., Vincenzi, F., & Castaldelli, G. (2019). Intense rainfalls trigger nitrite

- leaching in agricultural soils depleted in organic matter. *Science of The Total Environment*, 665, 80–90.
- Ngo, V. V., Michel, J., Gujisaite, V., Latifi, A., & Simonnot, M. (2014). Parameters describing nonequilibrium transport of polycyclic aromatic hydrocarbons through contaminated soil columns: Estimability analysis, correlation, and optimization. *Journal of Contaminant Hydrology*, 158, 93–109.
- Perović, M., Šenk, I., Tarjan, L., Obradović, V., & Dimkić, M. (2020). Machine learning models for predicting the ammonium concentration in alluvial groundwaters. *Environmental Modeling and Assessment*, 1, 1–17. <https://doi.org/10.1007/s10666-020-09731-9>
- Pot, V., Simlnek, J., Benoit, P., Coquet, Y., Yra, A., & Martinez-Cordon, M. J. (2005). Impact of rainfall intensity on the transport of two herbicides in undisturbed grassed filter strip soil cores. *Journal of Contaminant Hydrology*, 81(1–4), 63–88.
- Ramos, T. B., Šimůnek, J., Goncalves, M. C., Martins, J. C., Prazeres, A., Castanheira, N. L., & Pereira, L. S. (2011). Field evaluation of a multicomponent solute transport model in soils irrigated with saline waters. *Journal of Hydrology*, 407, 129–144.
- Sarioglu, M. (2005). Removal of ammonium from municipal wastewater using natural Turkish (dogantype) zeolite. *Separation and Purification Technology*, 41, 1–11.
- Šimůnek, J., & Van Genuchten, M. T. (2008). Modelling nonequilibrium flow and transport processes using Hydrus. *Vadoze Zone Journal*, 7(2), 782–797.
- Šimůnek, J., Sejna, M., Saito, H., Sakai, M., & van Genuchten, M. T. (2013). *The HYDRUS-1D software package for simulating the movement of water, heat, and multiple solutes in variably saturated media, version 4.17, HYDRUS software series 3* (p. 315). University of California Riverside, Riverside, California, USA.
- Sprynskyy, M., Lebedynets, M., Terzyk, A. P., Kowalczyk, P., Namiesnik, J., & Buszewski, B. (2005). Ammonium sorption from aqueous solutions by the natural zeolite Transcarpathian clinoptilolite studied under dynamic conditions. *Journal of Colloid and Interface Science*, 284, 408–415.
- Van Genuchten, M. T., & Wagenet, R. J. (1989). Two-site/two-region models for pesticide transport and degradation: Theoretical development and analytical solutions. *Soil Science Society of America Journal*, 53(5), 1303–1310.
- Wang, X. Y., Zhao, L., Liu, X. M. A. L. L., & Zhang, Y. X. (2013). Temperature effect on the transport of nitrate and ammonium ions in a loose-pore geothermal reservoir. *Journal of Geochemical Exploration*, 124, 59–66.
- Wang, Z., Li, J. S., & Li, Y. F. (2014). Simulation of nitrate leaching under varying drip system uniformities and precipitation patterns during the growing season of maize in the North China Plain. *Agricultural Water Management*, 142, 19–28.
- Wang, X. P., Huang, G. H., Yang, J. S., Liu, H. J., Huang, Q. Z., & Yu, L. P. (2015). An assessment of irrigation practices: Sprinkler irrigation of winter wheat in the North China Plain. *Agricultural Water Management*, 159, 197–208.
- Yan, X. Y., Ti, C. P., Vitousek, P., Chen, D., Leip, A., Cai, Z. C., & Zhu, Z. L. (2014). Fertilizer nitrogen recovery efficiencies in crop production systems of China with and without consideration of the residual effect of nitrogen. *Environmental Research Letters*, 9, 095002.
- Yang, L., Sun, T. T., Liu, Y. L., Guo, H. Q., Lv, L. X., Zhang, J., & Liu, C. (2017). Photosynthesis of alfalfa (*Medicago sativa*) in response to landfill leachate contamination. *Chemosphere*, 186, 743–748.
- Zhou, W., Ma, Y., Well, R., Wang, H., & Yan, X. (2018). Denitrification in shallow groundwater below different arable land systems in a high nitrogen-loading region. *Journal of Geophysical Research Biogeosciences*, 123, 991–1004.
- Zhou, L., Martin, S., Cheng, W., Lassabatere, L., Boily, J. F., & Hanna, K. (2019). Water flow variability affects adsorption and oxidation of ciprofloxacin onto hematite. *Environmental Science & Technology*, 53, 10102–10109.

**Publisher's Note** Springer Nature remains neutral with regard to jurisdictional claims in published maps and institutional affiliations.